Canine Placental Prostaglandin E2 Synthase: Expression, Localization, and Biological Functions in Providing Substrates for Prepartum PGF2alpha Synthesis 1

Authors: Gram, Aykut, Fox, Barbara, Büchler, Urs, Boos, Alois, Hoffmann, Bernd, et al.

Source: Biology of Reproduction, 91(6)

Published By: Society for the Study of Reproduction

URL: https://doi.org/10.1095/biolreprod.114.122929

BIOLOGY OF REPRODUCTION (2014) **91**(6):154, 1–14
Published online before print 8 October 2014.
DOI 10.1095/biolreprod.114.122929

Canine Placental Prostaglandin E2 Synthase: Expression, Localization, and Biological Functions in Providing Substrates for Prepartum PGF2alpha Synthesis[1]

Aykut Gram,[3] Barbara Fox,[3] Urs Büchler,[3] Alois Boos,[3] Bernd Hoffmann,[4] and Mariusz P. Kowalewski[2,3]

[3]*Institute of Veterinary Anatomy, Vetsuisse Faculty, University of Zurich, Zurich, Switzerland*
[4]*Clinic for Obstetrics, Gynecology and Andrology of Large- and Small Animals, Justus-Liebig University, Giessen, Germany*

ABSTRACT

The prepartum output of PGF2alpha in the bitch is associated with increased placental PGE2-synthase (PTGES) mRNA levels. Contrasting with this is a decreased expression of PGF2alpha-synthase (PGFS/AKR1C3) in uteroplacental compartments during prepartum luteolysis, suggesting an involvement of alternative synthetic pathways in PGF2alpha synthesis, for example, conversion of PGE2 to PGF2alpha. However, because the expression and possible functions of the respective PTGES proteins remained unknown, no further conclusion could be drawn. Therefore, a canine-specific PTGES antibody was generated and used to investigate the expression, cellular localization, and biochemical activities of canine uteroplacental PTGES throughout pregnancy and at prepartum luteolysis. Additionally, the biochemical activities of these tissues involved in the conversion of PGE2 to PGF2alpha were investigated. The endometrial PTGES was localized in the uterine surface epithelium at preimplantation and in superficial and deep uterine glands, endothelial cells, and myometrium throughout pregnancy and at parturition. Placental signals were mostly in the trophoblast. The biochemical properties of recombinant PTGES protein were confirmed. Additionally, expression of two PGE2-receptors, PTGER2/EP2 and PTGER4/EP4, revealed their decreasing expression during luteolysis. In contrast, the uteroplacental expression of prostaglandin transporter (PGT) was strongly elevated prior to parturition. These localization patterns resembled that of PTGES. The increased expression of PTGES and PGT at parturition, together with the accompanying decreased levels of PGE2-receptors and the capability of canine uterine and placental homogenates to take part in the conversion of PGE2 to PGF2alpha, as found in this study, suggest that PGE2 could be used locally as a substrate for prepartum PGF2alpha synthesis in the dog.

carnivore reproduction, comparative reproduction, female reproductive tract, pregnancy, prostaglandins

INTRODUCTION

The domestic dog is a nonseasonal, monoestrous animal that exhibits an obligatory sexual quiescence period (i.e., anestrus, between two consecutive estrous cycles). The endocrine and molecular mechanisms regulating reproduction in this species are still poorly understood. The corpus luteum (CL) is the main source of progesterone (P4) during canine pregnancy and in nonpregnant cycles [1] and is, therefore, required for the maintenance of pregnancy. Peripheral P4 secretion levels show similar patterns in both situations until shortly before parturition, when in pregnant animals, a steep P4 decline during prepartum luteolysis signals the onset of labor [1–4]. In contrast, in nonpregnant dogs, peripheral P4 concentrations continue to decrease progressively during a time span, lasting as much as 90 days, until levels of <1 ng/ml are reached, indicating the beginning of anestrus [5]. This slow luteal regression observed in nonpregnant dogs is independent of uterine luteolysin (PGF2α), and normal ovarian function is observed following hysterectomy [6]. Interestingly, based on the available evidence, the role of prostaglandins (PGs) produced within the CL must be considered relative to luteal maintenance rather than luteal regression/luteolysis [7–10].

Consequently, the gradually decreasing function of the CL in cyclic, nonpregnant dogs seems to be a passive process of slow luteal degeneration (reviewed in [11–13]). In strong contrast to this process is prepartum luteolysis, which is accompanied by an increase in the PGF2α-metabolite 13,14-dihydro-15-keto-PGF2α (PGFM) in maternal plasma [2, 3], indicating the luteolytic role of PGF2α. The placenta foetalis has been implicated as a possible source of this increase in PGF2α by clearly exhibiting expression of cyclooxygenase 2 (COX2, PTGS2) and PGF2α-synthase (PGFS/AKR1C3) in the fetal trophoblast [7, 14]. AKR1C3 is the only known canine-specific PGFS responsible for the enzymatic conversion of PGH2 to PGF2α [7]. Interestingly, whereas the expression of COX2 is upregulated prior to parturition, indicating strong activation of the PG system during this time, the expression of PGFS/AKR1C3 is reduced at both the mRNA and protein levels [14]. This reduction in PGFS/AKR1C3 expression is associated with decreased placental availability of 15-hydroxyprostaglandin dehydrogenase (HPGD; an enzyme catabolizing PGF2α and PGE2 to their inactive metabolites), which implies its contribution to the prepartum surge of PGF2α. Nevertheless, the decrease in uteroplacental PGFS/AKR1C3 expression implies that mechanisms not involving this enzyme might contribute to the prepartum release of PGF2α [14]. Accordingly, PGF2α can be synthesized by alternative biosynthetic cascades, using either PGE2 or PGD2 as substrates, due to the enzymatic activity of 9-keto-prostaglandin E2 reductase (9K-PGR, CBR1) or 11-keto-prostaglandin reductase (11K-PGR), respectively [15, 16]. In this regard, an interesting observation from our previous study [14] is the increased expression of

[1]Supported by Swiss National Science Foundation research grant 31003A_140947.
[2]Correspondence: Mariusz P. Kowalewski, Institute of Veterinary Anatomy, Vetsuisse Faculty, University of Zurich, Winterthurerstrasse 260, CH-8057 Zurich, Switzerland. E-mail: kowalewskipl@yahoo.de; or kowalewski@vetanat.uzh.ch

Received: 28 June 2014.
First decision: 3 August 2014.
Accepted: 2 October 2014.

eISSN: 1529-7268 http://www.biolreprod.org
ISSN: 0006-3363

PGE2-synthase (*PGES*, *PTGES*) mRNA in uteroplacental units at the time of both normal and antigestagen-induced parturition. PGE2-synthase mRNA expression was colocalized with increased expression of COX2 in fetal trophoblast, allowing us to speculate about the possible involvement of PGE2 in placental PGF2α synthesis. However, due to the lack of canine-specific antibodies, conclusions that could be drawn from that previous study were severely limited.

In the present study, a canine-specific antibody was generated, and the expression of PTGES was localized within canine uteroplacental compartments during the course of pregnancy from the preimplantation stage until prepartum luteolysis. The *PTGES* gene, which was cloned in our laboratory and deposited in GenBank under accession number NM_001122854 [9], is the only isoform of this enzyme so far described in the dog. Together with other PG synthases, it belongs to the aldo-ketoreductase family of enzymes. Its biochemical activity and subcellular localization were assessed in the present study, using heterogeneously expressed recombinant PTGES. Moreover, the reductive potential of uteroplacental homogenates contributing to the conversion of PGE2 to PGF2α was investigated. Additionally, in order to provide closer insights into possible autocrine and paracrine functions of PGE2 in uteroplacental tissues, the expression levels of PG transporter (PGT) and two PGE2 receptors (PTGER2/EP2 and PTGER4/EP4) were assessed.

MATERIALS AND METHODS

Tissue Collection and Preservation

All experimental procedures were carried out in accordance with animal welfare legislation and were approved by respective authorities of the Justus-Liebig University in Giessen, Germany, and University of Ankara, Turkey, where the tissue materials had been collected and used in our previous studies [7, 14, 17].

Tissue material was collected surgically by ovariohysterectomy (OHE), from 18 crossbred, healthy bitches, 2–8 yr of age, which were included in the study and allotted to 4 experimental groups according to stage of pregnancy: preimplantation (Days 8–12, n = 5), postimplantation (Days 18–25, n = 5), mid-gestation (Days 35–40, n = 5), and prepartum luteolysis (n = 3). The mating day was designated as Day 0 of pregnancy for all bitches and was 2–3 days after ovulation, which was assessed by measurements of P4 (>5 ng/ml in peripheral blood) and by evaluation of vaginal smears. Preimplantation status was verified by detecting the presence of embryos in uterine flushings, with a stereomicroscope. According to descriptions by Amoroso [18] and Kehrer [19], the postimplantation and mid-gestation stages of canine pregnancy are characterized by the formation or presence, respectively, of fully developed uteroplacental compartments. The day of prepartum luteolysis was detected by regular measurements of peripheral P4 concentration at 6-h intervals beginning with Day 58 of gestation; OHE was performed after maternal P4 concentrations dropped below 3 ng/ml in 2 consecutive measurements.

For immunohistochemistry (IHC) and nonradioactive in situ hybridization (ISH), uterine samples (at preimplantation stage of pregnancy) were collected immediately after OHE. Following implantation, uteroplacental compartments, understood as full thickness, middle part of the girdle, avoiding the marginal hematoma, were collected. All tissues were cleaned of surrounding connective tissues and fixed with 10% neutral phosphate-buffered formalin for 24 h at +4°C. Then, samples were washed daily with fresh phosphate-buffered saline (PBS) for 1 wk, dehydrated in a graded ethanol series, and embedded in a paraffin equivalent Histo-Comp (Vogel, Giessen, Germany). For total RNA isolation and Western blotting applications, samples from the uterus and uteroplacental compartments were immersed in RNAlater (Ambion Biotechnology GmbH, Wiesbaden, Germany) for 24 h at +4°C and subsequently stored at −80°C until analysis.

Construction of PTGES Expressing EYFP- and His-Tagged Plasmids

The Gateway cloning technology (Invitrogen, Carlsbad, CA) was used for cloning of PTGES expression plasmids according to the manufacturer's protocol and as described previously [7]. Briefly, using the canine-specific sequence of *PGES* (*PTGES*) as a template (GenBank accession number NP_001116326; *Canis lupus* familiaris prostaglandin E synthase [*PTGES*] mRNA, complete cds) [9], primers were designed, including attB sequences that were attached to forward and reverse oligonucleotides to amplify open reading frame, including PCR products suitable for BP recombination. The stop codon was removed from the reverse primer in order to enable the subsequent synthesis of fusion protein-expressing constructs. The following sequences were used (regions showing gene-specific sequences are in boldface type): attB1-*PTGES* forward, 5′-GGG GAC AAG TTT GTA CAA AAA AGC AGG CTT A**AT GCC TCC CCC TGT CCT GGC**; and attB2-*PTGES* reverse, GGG GAC CAC TTT GTA CAA GAA AGC TGG GTT **CAG GTG GCA GGC TGC TTC CC**.

The PCR reaction was run with Phusion High-Fidelity DNA hot start polymerase (New England Biolabs, Frankfurt, Germany) in an Eppendorf Mastercycler (Vaudaux-Eppendorf AG, Basel, Switzerland) under conditions previously described [7]. After purification with a gel extraction system (Qiaex II; Qiagen GmbH, Hilden, Germany), the attB-flanked PCR products were used for BP recombination with attP-containing pDONOR221 vector with BP clonase II. The entry clone obtained was amplified in One Shot ccdB Survival 2 T1R-competent cells (Invitrogen) on kanamycin-containing agar plates and purified using the PureYield Plasmid Miniprep System (Promega, Dübendorf, Switzerland). Afterward, entry clones containing attL sites were recombined with pHSV-EYFP-Rfc-C1 and pHSV-V5His-Rfc-C1 expression vectors [20] in the presence of LR clonase II (Invitrogen) to produce plasmids expressing the EYFP (Enhanced Yellow Fluorescent Protein) and His-tagged canine-specific PTGES fusion proteins. The generated expression vectors were amplified in One Shot ccdB Survival 2 T1R Competent Cells (Invitrogen), purified with the PureYield Plasmid Miniprep System (Promega), control digested to confirm the presence of insert, and finally commercially sequenced on both strands (Microsynth, Balgach, Switzerland).

Transient Expression and Subcellular Localization of Recombinant PTGES Protein

The Vero 2.2 cell line served as a heterologous system according to the previously described protocol [7]. Cells were cultured in Dulbecco Modified Eagle Medium-high glucose (Chemie Brunschwig AG, Basel, Switzerland) containing 2 mM L-glutamine, heat-inactivated 2% fetal bovine serum (Chemie Brunschwig AG), and 1% penicillin-streptomycin (Chemie Brunschwig) in humidified air containing 5% CO_2 at 37°C. Transfection of pHSV-EYFP-Rfc-C1-PTGES and pHSV-V5His-Rfc-C1-PTGES expression vectors was achieved with FuGENE HD-transfection reagent (Roche Diagnostics, Mannheim, Germany) at a ratio of 1 μg of DNA to 3.5 μl of reagent. Transfection efficiency was checked by inspecting the pHSV-EYFP-Rfc-C1-PTGES-transfected cells under a fluorescent microscope. For subsequent Western blot analysis, cells were washed with ice-cold sterile PBS and harvested using a NET-2 lysis buffer (50 mM Tris-HCl, pH 7.4, 300 mM NaCl, 0.05% NP-40) containing protease inhibitor cocktail (10 μl/ml; Sigma-Aldrich, Chemie GmbH, Buchs, Switzerland).

The subcellular localization of PTGES-EYFP recombinant proteins was assessed in cells grown on sterile cover glasses, using a Leica SP2 model confocal microscope (Leica Microsystems AG, Heerbrugg, Switzerland). Cells transiently expressing the fluorescent recombinant proteins were fixed with formaldehyde (2% final concentration) for 10 min at 37°C. For permeabilization, PBS-0.1% Triton X-100 was used for 2 min at room temperature, followed by 3 washing steps of 5 min each with PBS. Cells were then incubated for 20 min at room temperature with the respective conjugates (i.e., Alexa Fluor 594-conjugated concanavalin A [20 μg/ml; Invitrogen]) for detecting endoplasmic reticulum (ER) or with Alexa Fluor 633-conjugated wheat germ agglutinin (5 μg/ml; Molecular Probes, Inc., Leiden, Netherlands) for detecting Golgi apparatus. Then, 4′,6-diamidino-2-phenylindole (DAPI; Sigma-Aldrich) was added to the conjugate solution to achieve nuclear staining. Cells were then washed 3 times for 10 min each with H_2O at room temperature. Finally, cover glasses with cells were mounted with Glycergel (Dako North America, Inc., Carpinteria, CA) on microscope slides, and signals were visualized using confocal microscopy.

Purification of PTGES-His-Tagged Recombinant Protein, Its Enzymatic Activity, and Determination of the Biochemical Potential of Uteroplacental Homogenates to Assist in the Conversion of PGE2 to PGF2α by 9K-PGE2 Reductase Activity

Heterogeneously expressed His-tagged PTGES protein was purified with nickel-nitrilotriacetic acid magnetic agarose beads (Qiagen), using the

manufacturer's protocol. An ER isolation kit (Sigma-Aldrich) was used, following the provider's instructions, to isolate microsomal fractions from tissue homogenates obtained from dogs during prepartum luteolysis. Placental and uterine tissue compartments were separated macroscopically and then subjected to the experimental procedure.

The biochemical activities of the recombinant PTGES, as well as that of the uteroplacental microsomes, were determined by applying a recently elaborated protocol [7], with some minor modifications. NADPH (1.0 μM [Sigma-Aldrich]) was used as a cofactor in reactions containing 0.5 μg recombinant protein or uterine and placental microsomal fractions in 100 μl of 50 mM Tris HCl, pH 7.5. As a substrate, 0.001–0.1 μM PGH2 or PGE2 was used. For negative controls, reactions were performed omitting proteins, and detected background signals were subtracted from the readouts obtained in experiments run with proteins. Assays were carried out at 37°C for 1–10 min. Each experiment was repeated at least three times. The following enzymatic conversions were assessed: PGH2 into PGE2 and PGF2α for the PTGES recombinant protein, and PGE2 to PGF2α for the uterine and placental homogenates. The PGF2α and PGE2 enzyme immunoassay kits (Cayman Chemical Co., Ann Arbor, MI) were used according to the manufacturer's instructions. The intra- and interassay coefficient of variation values were approximately 3%. In a final step, plates were read photometrically using a SpectraMax Plus384 absorbance microplate reader (Bucher Biotec AG, Basel, Switzerland) set at 405 nm.

Protein Preparation and Western Blot Analysis

Protein extraction and SDS-PAGE were performed according to our previously published protocol [21–23]. The NET-2 lysis buffer containing 10 μl/ml protease inhibitor cocktail (Sigma-Aldrich) was used for protein preparation. Proteins were electroblotted onto polyvinylidene difluoride membranes (Bio-Rad Laboratories, Inc., Hercules, CA). The horseradish peroxidase (HRP)-conjugated secondary antibodies were detected with Immun-Star Western C chemiluminescent kit substrate (Bio-Rad) and SuperSignal West Femto Chemiluminescent Substrate (Pierce Biotechnology, Rockford, IL) according to the manufacturers' protocols. Finally, immunoreactive bands were detected using ChemiDoc XRS+ System and Image Lab (Bio-Rad).

Canine-specific guinea pig polyclonal affinity-purified anti-PTGES antibody was generated (Eurogentec SA, Seraing, Belgium) against RSDQDVDRCLRAHRND-C terminal amino acids 61–76 of the canine PTGES protein (GenBank accession no. NP_001116326). Antibody was applied at a 1:25 dilution in the Western blot analysis. Additional antibodies used for this study were rabbit polyclonal, affinity-purified immunoglobulin G (IgG) against EP2 (1:500 dilution) and EP4 (1:500 dilution), together with respective blocking peptides (Cayman Chemical Co.); mouse monoclonal anti-EYFP (1:1000 dilution; product no. 632380; code JL-8; Clontech Laboratories, Saint-Germain-en-Laye, France); monoclonal mouse anti-His (product no. R940-25; 1:100 dilution; Invitrogen); mouse monoclonal anti-β-actin antibody (code sc-69879; 1:1000 dilution; Santa Cruz Biotechnology, Dallas, TX); secondary HRP goat anti-mouse IgG (1:15 000; code W402B; Promega); secondary donkey anti-rabbit HRP-labeled secondary IgG (1:15 000; Pierce Biotechnology, Rockford, IL); and anti-guinea pig IgG conjugated to HRP (code A5545; 1:15 000; Sigma-Aldrich).

Semiquantitation of PTGER2 (EP2) and PTGER4 (EP4) protein expression levels was achieved by reblotting the Western blot membranes with anti-β-actin antibody, used as a loading control. ImageJ software (US National Institutes of Health, Bethesda, MD) was applied to determine the optical density of bands. The values are presented as the ratio of target protein optical density to β-actin optical density.

Immunohistochemistry

The IHC procedure was performed using our standard immunoperoxidase method as reported previously [10, 23]. Briefly, formalin-fixed paraffin-embedded tissues were cut (2–3 μm), mounted on microscope slides (Super Frost; Menzel-Glaeser, Braunschweig, Germany), deparaffinized in xylene, rehydrated in a graded ethanol series, and washed under running tap water. For antigen retrieval, slides were preincubated in 10 mM citrate buffer, pH 6.0, at room temperature prior to microwave irradiation at 560 W for 15 min. Endogenous peroxidase activity was quenched by immersing the sections in 0.3% hydrogen peroxide in methanol. Nonspecific binding sites were blocked by incubation with either 10% horse serum or 10% normal goat serum, depending on the secondary antibody used. Then, respective primary antibodies were applied overnight at +4°C. The primary antibodies used for IHC were canine-specific guinea pig polyclonal affinity purified anti-PTGES (the same as those used for Western blotting; 1:300 dilution; Eurogentec); rabbit polyclonal anti-EP2 (1:200 dilution), and anti-EP4 (1:100 dilution; Cayman Chemical Co.); goat polyclonal affinity purified anti-PGT IgG (1:100 dilution; Santa Cruz Biotechnology); monoclonal mouse anti-vimentin (1:100 dilution) and polyclonal rabbit anti-cytokeratin (1:300 dilution; Dako). Samples omitting the primary antibody and antiserum-specific isotype controls applied at the same dilution and protein concentration as the primary antibody served as negative controls. The following secondary antibodies were used for 30 min at room temperature at 1:100 dilution: biotinylated goat anti-guinea pig IgG BA-7000; goat anti-rabbit IgG BA-1000; horse anti-goat IgG BA-9500; and horse anti-mouse IgG BA2000 (all from Vector Laboratories Inc., Burlingame, CA). Subsequently, slides were incubated for 30 min with the streptavidin-peroxidase Vectastain ABC kit (Vector Laboratories) to enhance the signals. Peroxidase activity was detected using liquid DAB+ substrate kit (Dako). Slides were counterstained with hematoxylin and mounted in Histokit (Assistant, Osterode, Germany).

Total RNA Isolation and Real-Time (TaqMan) PCR

Total RNA extraction was performed using TRIzol reagent (Invitrogen) following the manufacturer's protocol. Concentrations of RNA were determined with a NanoDrop 2000C spectrophotometer (Thermo Fisher Scientific AG, Reinach, Switzerland). Genomic DNA contamination was removed with the RQ1 RNase-free DNase (Promega) following the manufacturer's instructions. Reverse transcription was carried out using random hexamers as primers and other reagents (Applied Biosystems, Foster City, CA) as previously reported [10, 17].

The expression of *PGT* mRNA in the preimplantation uterus and uteroplacental compartments during pregnancy and normal and induced parturition were analyzed by real-time (TaqMan) PCR using an automated fluorimeter ABI PRISM 7500 Sequence Detection System (Applied Biosystems). The previously described protocol was applied [10, 17]. Each sample was analyzed in duplicate. Autoclaved water instead of cDNA and the so-called minus-reverse transcription controls were run for negative controls. Reactions were set up in mixtures consisting of 200 nM TaqMan probe, 300 nM of each primer, 12.5 μl of Fast Start universal probe Master (ROX; Roche Diagnostics); and 5 μl of cDNA, corresponding to 100 ng total RNA. The cycling conditions were denaturation at 95°C for 10 min, 40 cycles at 95°C for 15 sec, and 1 cycle at 60°C for 60 sec. *GAPDH*, *18S* rRNA, and cyclophilin A (*PPIA*) were used for normalization of target gene expression in the comparative cycle threshold method (ΔΔCT), ensuring approximately 100% reaction efficiency, according to the manufacturer's protocols for the ABI PRISM 7500 Sequence Detection System and as described previously [10, 17]. The relative gene expression was calculated using the sample with the lowest concentration of target gene as a calibrator.

The primers and probes for *PGT*, *GAPDH*, and *18S* rRNA were designed based on the canine-specific sequences of *PGT* (GenBank accession number NM_001011558), *GAPDH* (GenBank accession number AB028142), and *18S* rRNA (GenBank accession number FJ797658). The sequences of primers and probes were *PGT* forward: 5′-TGC AGC ACT AGG AAT GCT GTT C-3′; *PGT* reverse: 5′-GGG CGC AGA GAA TCA TGG A-3′; *PGT* TaqMan probe: 5′-TCT GCA AAC CAT TCC CCG CGT G-3′ (length of the amplicons was 116 base pairs [bp]); *GAPDH* forward: 5′-GCT GCC AAA TAT GAC GAC ATC A-3′; *GAPDH* reverse: 5′-GTA GCC CAG GAT GCC TTT GAG-3′; *GAPDH* TaqMan probe: 5′-TCC CTC CGA TGC CTG CTT CAC TAC CTT-3′ (length of the amplicons was 75 bp); *18S* rRNA forward: 5′-GTC GCT CGC TCC TCT CCT ACT-3′; *18S* rRNA reverse: 5′-GGC TGA CCG GGT TGG TTT-3′; *18S* rRNA TaqMan probe: 5′-ACA TGC CGA CGG GCG CTG AC-3′ (length of amplicons was 125 bp). A commercially available gene-specific TaqMan probe and primer sets of canine-specific cyclophilin A (TaqMan system) were purchased from Applied Biosystems (product no. Cf03986523-gH). Selected PCR products were commercially sequenced (Microsynth) in order to confirm the specificity of amplicons.

In Situ Hybridization

The expression of *PGT* was additionally localized in the canine uteroplacental compartments at the mRNA level by using a nonradioactive ISH method with formalin-fixed paraffin-embedded sections as described previously [23]. The 348-bp PCR product, amplified with the following primers: *PGT* forward: 5′-GGA TGA AGC AAG GAA GAT G-3′; and *PGT* reverse: 5′-ATG GAG ATG GTG ATG ATG G-3′, served as the template for synthesis of the digoxigenin (DIG)-labeled cRNA probes. Detection of DIG-labeled riboprobes was done after incubating slides with alkaline phosphatase-conjugated, sheep anti-DIG Fab fragments (Roche Diagnostics) diluted 1:5000. Signals were detected using the substrate 5-bromo-4-chloro-3-indolyl phosphate and Nitroblue Tetrazolium (NBT/BCIP; Roche Diagnostics).

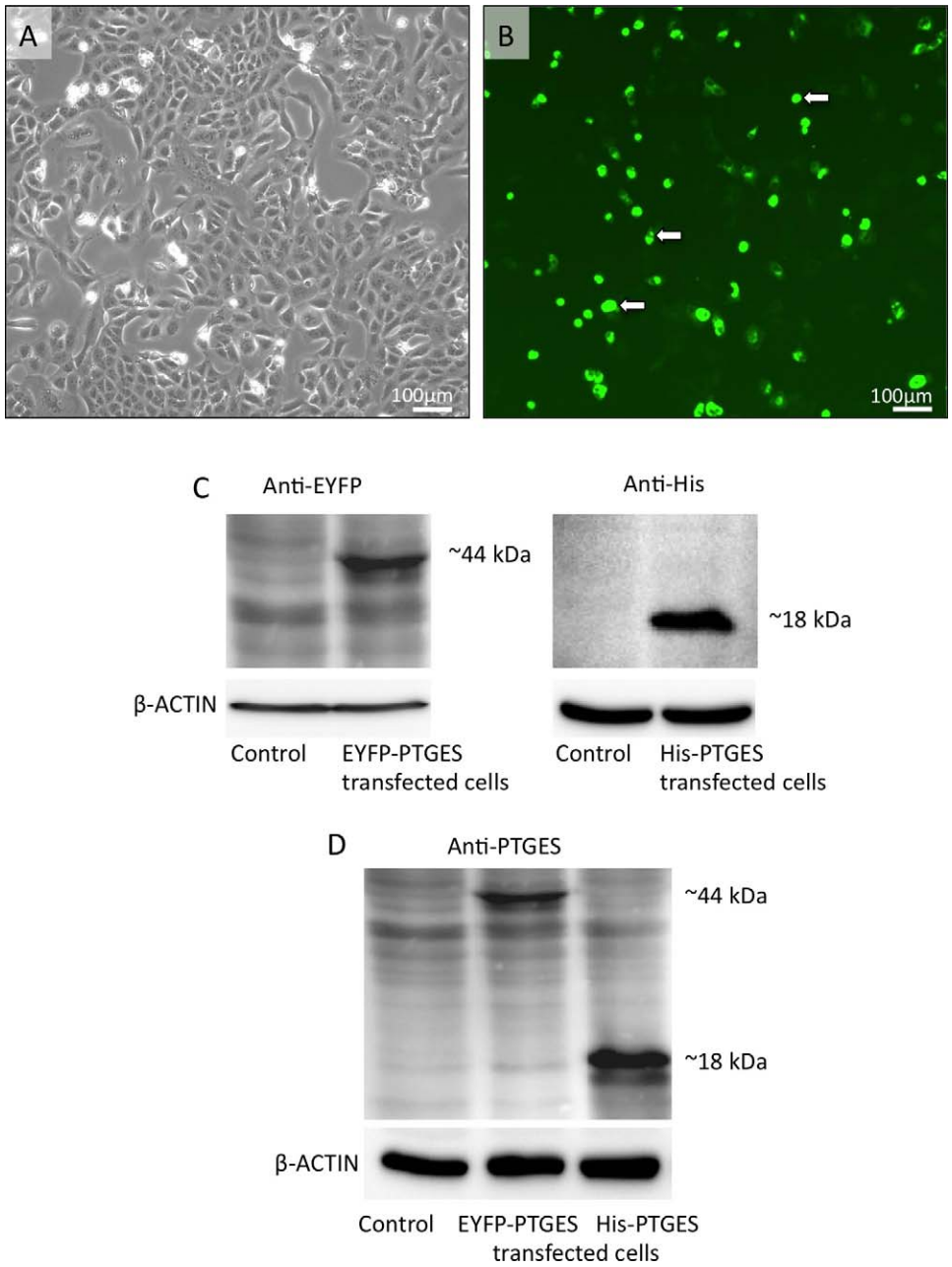

FIG. 1. Transfection of Vero 2.2 cells with pHSV-EYFP-Rfc-C1-PTGES (for EYFP-PTGES recombinant fusion-protein expression) and pHSV-V5His-Rfc-C1-PTGES (for His-PTGES recombinant fusion-protein expression) vectors. Validation of canine-specific anti-PGES antibody. **A**) Brightfield microscopy view of Vero 2.2 cells 24 h after transfection. **B**) pHSV-EYFP-Rfc-C1-PTGES expression in transfected Vero 2.2 cells. White arrows indicate fluorescing cells expressing EYFP-PTGES (green). **C**) Expression of EYFP-PTGES (~44 kDa) and His-PTGES (~18 kDa) fusion proteins in Vero 2.2 cell lysates was analyzed by Western blot analysis using anti-EYFP and anti-His antibodies. A lysate from nontransfected Vero 2.2 cells was used as a negative control; β-actin expression (45 kDa) served as a loading control. **D**) Western blot analysis of His-PTGES and EYFP-PTGES recombinant protein expression in Vero 2.2 cell lysates stained with custom-made canine-specific anti-PTGES antibody; nontransfected Vero 2.2 cells were used as negative control, and β-actin (45 kDa) was used as an internal loading control.

Data Evaluation

The effects of time on *PGT* mRNA expression and PTGER2 (EP2) protein expression were assessed by applying a parametric one-way analysis of variance (ANOVA), followed by a Tukey-Kramer multiple comparisons post-test. Due to the uneven distribution of the data obtained for PGTER4 (EP4) protein expression, the Kruskal-Wallis test (a nonparametric ANOVA) followed by Dunn multiple comparison test was performed. Numerical data are presented as means ± standard deviations (S.D.). GraphPad version 3.06 software (GraphPad Software, San Diego, CA) was used. A P value of <0.05 was considered statistically significant.

RESULTS

Expression and Localization of PTGES in Canine Uteroplacental Compartments at Selected Time Points During Pregnancy and at Prepartum Luteolysis

The pHSV-EYFP-Rfc-C1-PTGES and pHSV-V5His-Rfc-C1-PTGES vectors were transfected into Vero 2.2 cells, which served as a heterologous expression system for synthesis of recombinant canine EYFP-tagged and His-tagged PTGES

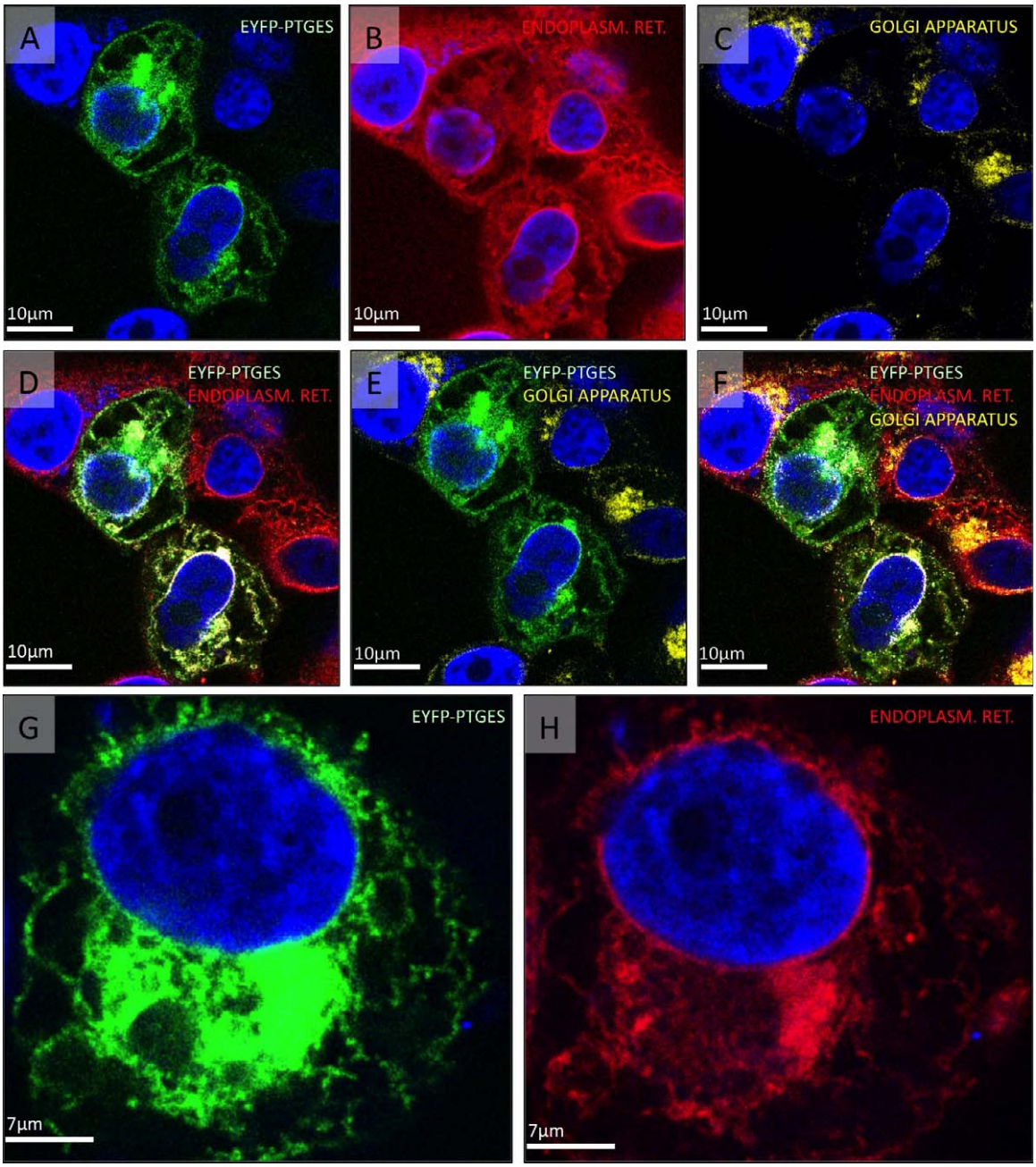

FIG. 2. Subcellular localization of EYFP-PTGES recombinant protein in pHSV-EYFP-Rfc-C1-PTGES-transfected Vero 2.2 cells. Endoplasmic reticulum (ER) was detected by concanavalin A staining and Golgi apparatus was visualized by wheat germ agglutinin staining. **A**) Expression of canine recombinant EYFP-PTGES fusion protein (green). **B**) ER (red) is shown. **C**) Golgi apparatus (yellow). **D**) EYFP-PTGES/ER merged image indicate the localization of PTGES to microsomes. **E**) EYFP-PTGES/Golgi apparatus merged image; there is no overlapping. **F**) EYFP-PTGES/ER/Golgi apparatus merged image. **G** and **H**) Higher magnification shows the subcellular localization of recombinant EYFP-PTGES fusion protein (**G**) and ER (**H**). Nuclear staining was achieved with DAPI (see *Materials and Methods*).

proteins. Transfection efficiency was assessed by monitoring the cellular expression of fluorescent EYFP-PTGES protein (Fig. 1, A and B). Cells were harvested when high transfection efficiency was detected, approximately 24–48 h after transfection, and cell lysates were used in Western blot analysis. Anti-His and anti-EYFP antibodies were used, allowing estimation of the molecular weight of both proteins. Whereas the PTGES-EYFP protein was detected as an immunoreactive band of approximately 44 kDa, the actual size of canine PTGES, determined based on the His-tagged protein molecular weight, was approximately 18 kDa (Fig. 1C). In the next step, the recombinant cell homogenates were probed with the new custom-made anti-PTGES antibody, revealing results similar to those obtained with the anti-EYFP and anti-His antibodies and confirming its specificity (Fig. 1D). In all experiments, nontransfected control Vero cells were used as a negative control, displaying background staining that could be differentiated from the positive signals achieved with the specific antibodies. The efforts to detect Western blot PTGES signals in the native tissue homogenates obtained from uteroplacental compartments from different gestational stages failed, which presumably can be attributed to the lower detection limit of the antibody in these complex tissue homogenates.

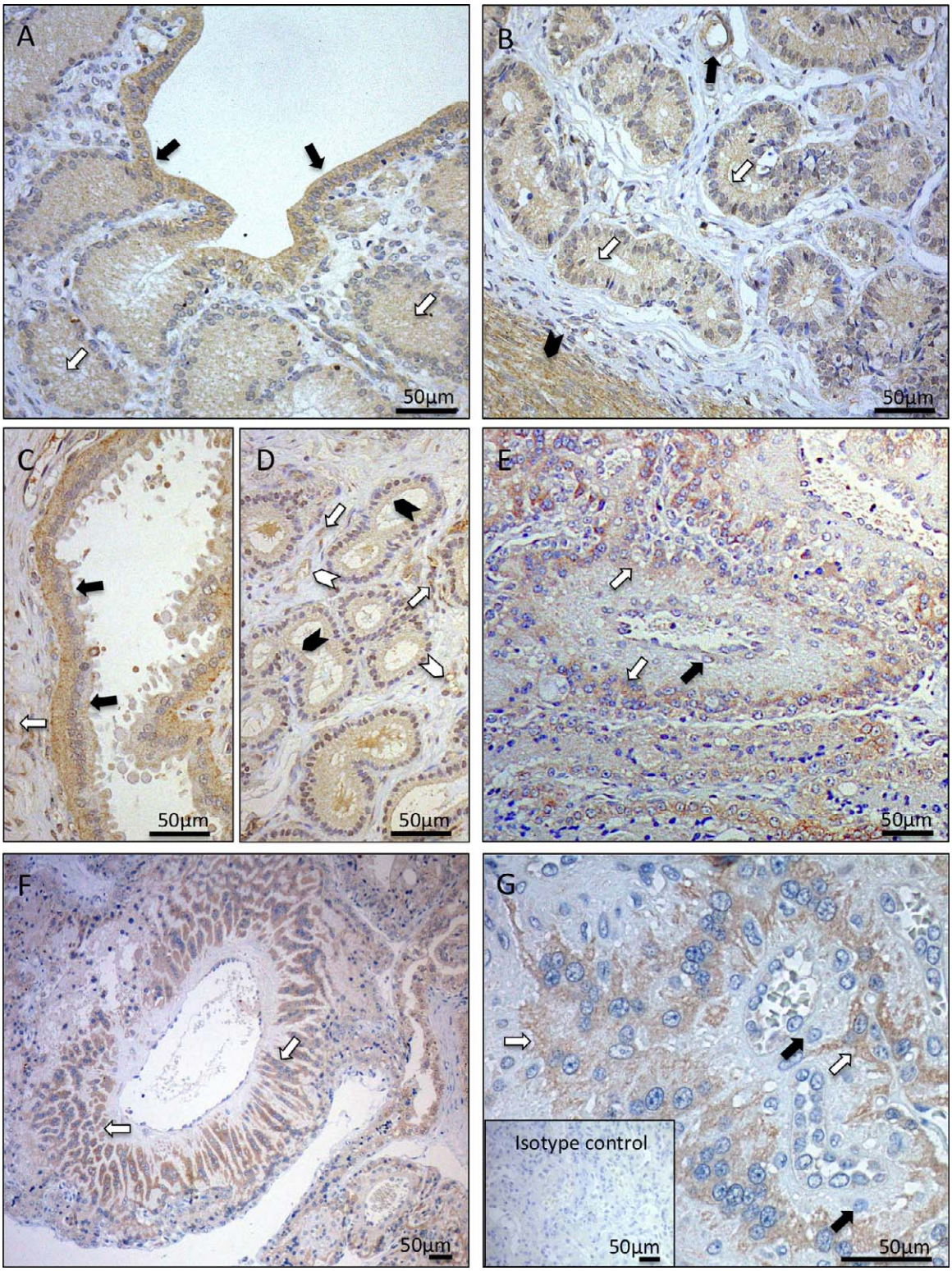

FIG. 3. Immunohistochemical localization of PTGES in the canine early pregnant uterus and uteroplacental compartments at selected time points during pregnancy: at the preimplantation stage (**A** and **B**), in the uteroplacental compartments at midgestation (**C**, **D**, and **E**), and in the uteroplacental compartments during prepartum luteolysis (**F** and **G**). **A** and **B**) Preimplantation PTGES is localized to the surface (luminal) epithelial cells (solid arrows [**A**]), glandular epithelial cells of the superficial and deep uterine glands (open arrows [**A** and **B**]), myocytes (solid arrowhead [**B**]), and vascular endothelial cells (solid arrow [**B**]). After implantation, within the uteroplacental compartments, endometrial signals are localized to the superficial uterine glands (the so-called glandular chambers) (solid arrows [**C**]), deep uterine glands (solid arrowheads [**D**]), endometrial stromal cells (open arrow [**C** and **D**]), and vascular endothelial cells (open arrowheads [**D**]). In the placental labyrinth, fetal trophoblast cells stain strongly (open arrows [**E**, **F**, and **G**]), and maternal decidual cells stain weakly (solid arrows [**E** and **G**]) for PTGES. There is no background staining in the isotype control (inset [**G**]).

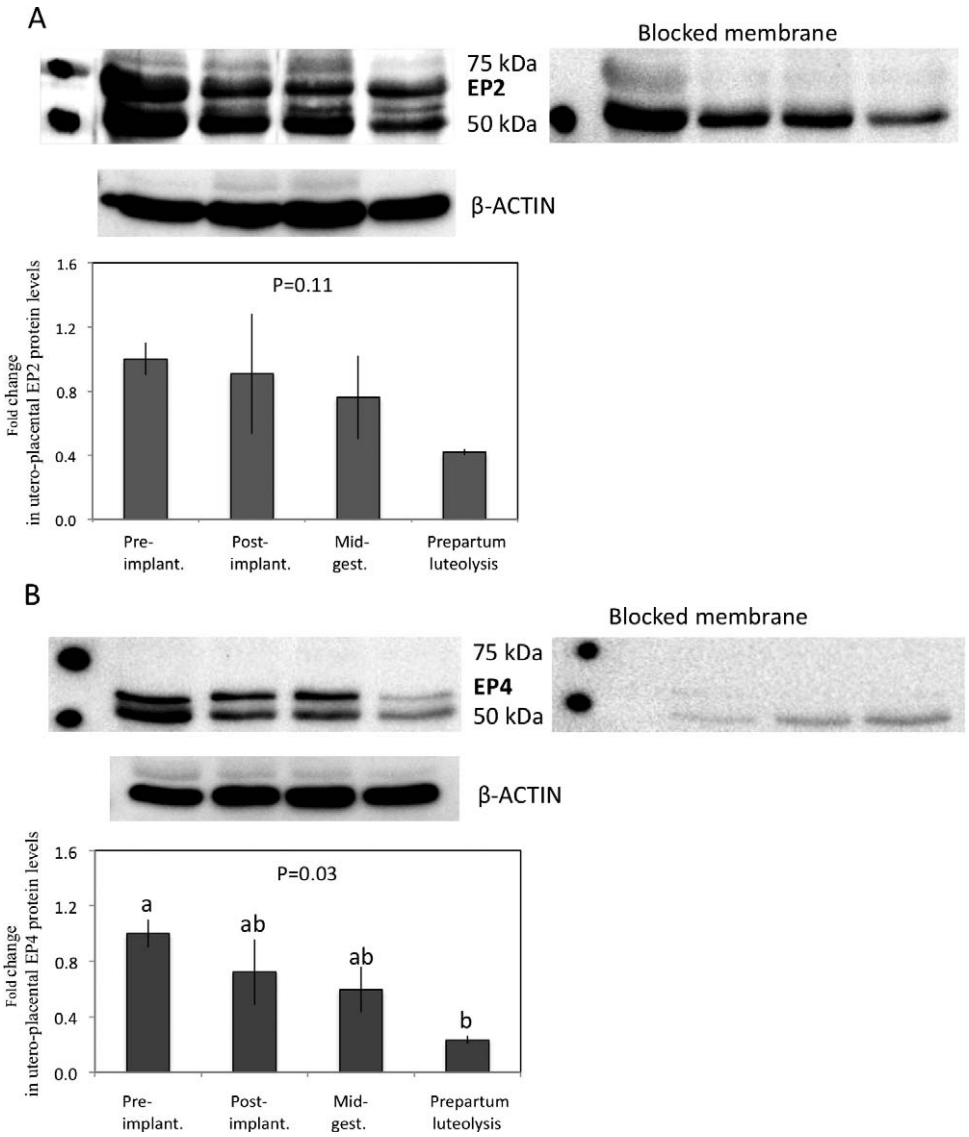

FIG. 4. Expression of PTGER2/EP2 (**A**) and PTGER4/EP4 (**B**) proteins in uteroplacental units throughout pregnancy was detected by Western blot analysis. Epitope-blocking peptide was used for both antibodies in order to block specific EP2 and EP4 signals. Representative immunoblots are shown. β-actin (45 kDa) served as the internal loading control.

The subcellular localization of PTGES-EYFP recombinant protein was visualized using confocal microscopy (Fig. 2). In order to differentiate between the different cellular components, ER was detected by concanavalin A staining, and Golgi apparatus was revealed by wheat germ agglutinin staining. The localization of heterogeneously expressed PTGES-EYFP matched the concanavalin A staining, indicating association of the recombinant protein with the ER (Fig. 2). No overlapping was observed for the expression of PTGES-EYFP and staining of the Golgi apparatus.

As determined by IHC, prior to implantation, PTGES was predominantly localized in the uterine surface (luminal) epithelial cells, superficial and deep uterine glands, and myometrium (Fig. 3, A and B). Staining was also visible in vascular endothelial cells. Weaker signals were detected in uterine stromal cells. Following placentation and at mid-gestation, similar uterine localization at placentation sites was seen, with distinctly stronger signals observed in the superficial uterine glands enlarging to the so-called glandular chambers than in the deep uterine glands (Fig. 3, C and D). In the clearly visible placental labyrinth, intense signals were localized in the fetal trophoblast cells from postimplantation until prepartum luteolysis (Fig. 3, E–G). No signals or only weak signals were detectable in the maternal part of the placenta, the so-called decidual cells (Fig. 3, E–G).

Biochemical Activities of Canine PTGES and 9K-PGR Activity of Uteroplacental Homogenates

Canine PTGES-His-tagged fusion protein and the uterine and placental microsomal fractions were purified as described in *Materials and Methods*. Canine PTGES revealed synthetic activity toward conversion of PGH2 to PGE2 but not toward PGF2α, thereby confirming its biochemical identity. The maximal enzymatic activity, yielding 10.22 ± 2.72 ng/μg protein, was observed with 0.1 μM PGH2 within 10 min. Under the same experimental conditions, the microsomal fractions isolated from uteroplacental compartments during prepartum luteolysis showed the maximum conversion rate of PGE2 to PGF2α, displaying values of 22.8 ± 4.48 ng/μg

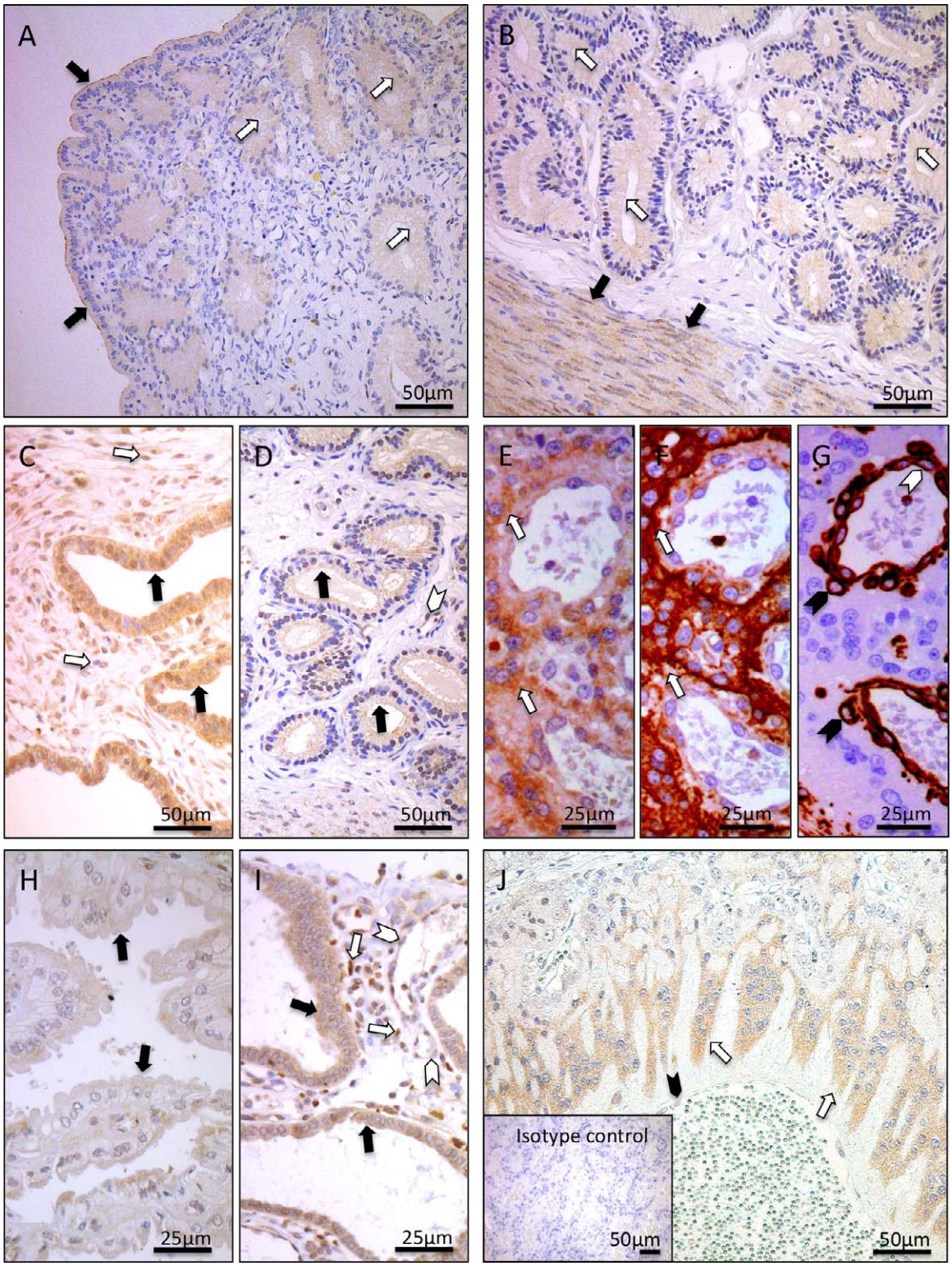

FIG. 5. Immunohistochemical localization of PTGER2/EP2 in the canine pregnant uterus throughout pregnancy. At the preimplantation stage (**A** and **B**), in the uteroplacental compartments at midgestation (**C**, **D**, and **E**), and in the uteroplacental compartments during prepartum luteolysis (**H**, **I**, and **J**). **A** and **B**) Preimplantation endometrial PTGER2/EP2 expression is localized to the surface (luminal) epithelial cells (solid arrows [**A**]), glandular epithelial cells of the superficial and deep uterine glands (open arrows [**A** and **B**]) and myocytes (solid arrows [**B**]). Following implantation, within the uteroplacental compartments, endometrial signals are localized to the superficial uterine glands (the so-called glandular chambers) and epithelial cells of the deep uterine glands (solid arrows [**C** and **D**]), endometrial stromal cells (open arrow [**C**]), and vascular endothelial cells (open arrowheads [**D**]). A similar localization pattern is observed during prepartum luteolysis in the endometrium: superficial endometrial glands (glandular chambers) and deep uterine glands (solid arrows [**H** and **I**]), endometrial stromal cells (open arrows [**I**]), and vascular endothelial cells (open arrowheads [**I**]). In the placental labyrinth, fetal trophoblast cells stain strongly (open arrows [**E** and **J**]) for PTGER2/EP2. Solid arrowhead in **J** indicates maternal endothelial cells. The detection of cytokeratin (**F**) and vimentin (**G**) was performed in consecutive sections in order to more easily differentiate cell types within the canine placenta, i.e., endothelial, trophoblast, and decidual cells. Trophoblast cells stain positively for cytokeratin (open arrows [**F**]), while endothelial cells (open arrowheads [**G**]) and decidual cells (solid arrowheads [**G**]) stain positively for vimentin. There is no background staining in the isotype control (inset [**J**]).

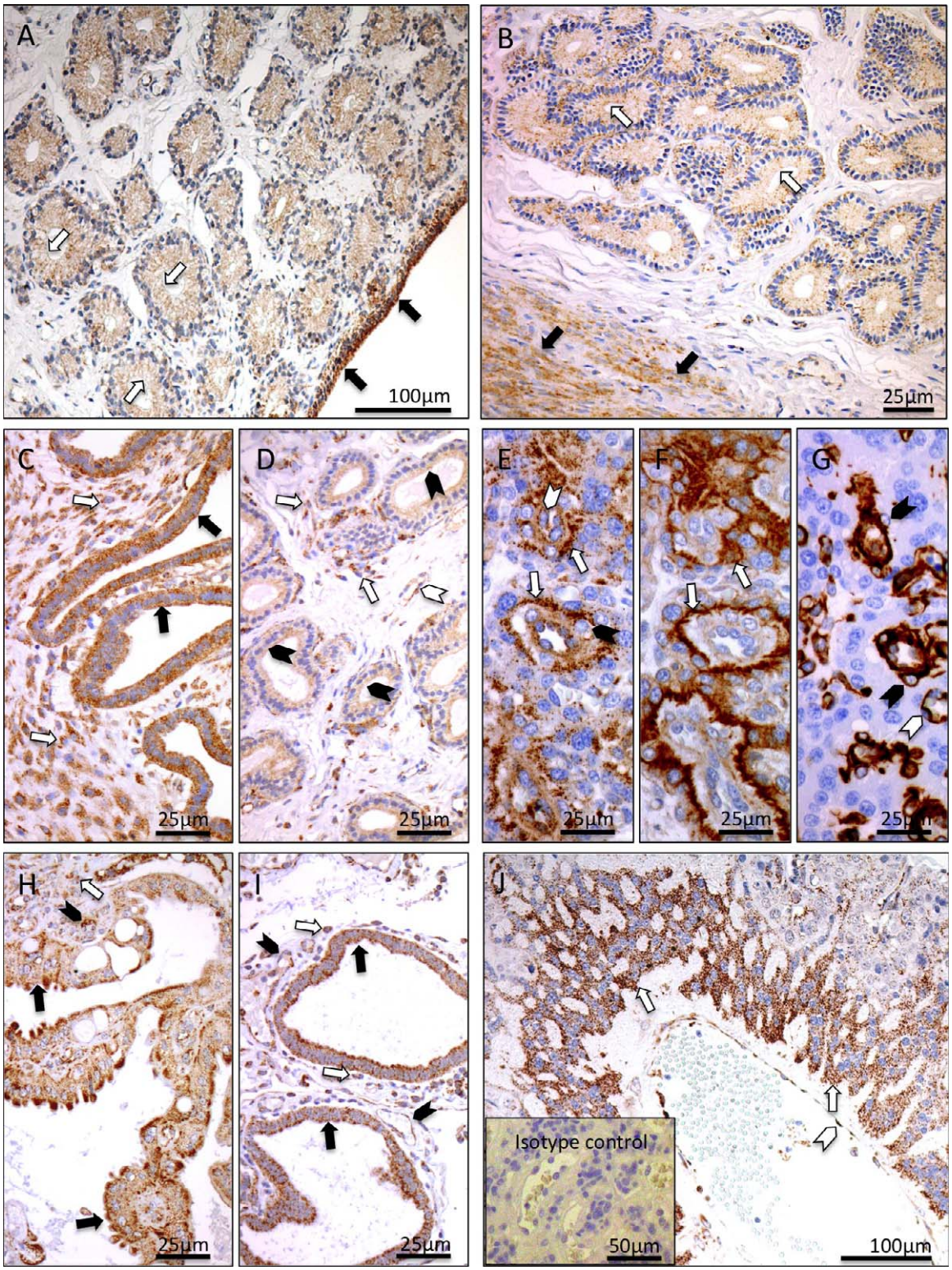

FIG. 6. Immunohistochemical localization of PTGER4/EP4 in the canine pregnant uterus at selected periods of pregnancy: at the preimplantation stage (**A** and **B**), in the uteroplacental compartments postimplantation (**C**, **D**, and **E**), and in the uteroplacental compartments during prepartum luteolysis (**H**, **I**, and **J**). **A** and **B**) Preimplantation endometrial PTGER4/EP4 expression is localized to the surface (luminal) epithelial cells (solid arrows [**A**]), glandular epithelial cells of the superficial and deep uterine glands (open arrows [**A** and **B**]) and myocytes (solid arrows [**B**]). Following implantation, within the uteroplacental compartments, endometrial signals are localized to the superficial uterine glands (the so-called glandular chambers) (solid arrows [**C**]), epithelial cells of the deep uterine glands (solid arrowheads [**D**]), endometrial stromal cells (open arrows [**C** and **D**]), and vascular endothelial cells (open arrowheads [**D**]). Strong endometrial signals are also observed during prepartum luteolysis: in the superficial endometrial glands (glandular chambers) (solid arrows [**H**), deep uterine glands (solid arrows [**I**]), endometrial stromal cells (open arrows [**H** and **I**]), and vascular endothelial cells (solid arrowheads [**H** and **I**]). In the placental labyrinth, invading trophoblast at the base of the placental labyrinth surrounding maternal blood vessels (open arrows [**E** and **J**]) and maternal endothelial cells (open arrowheads [**E** and **J**]) stain positively for EP4. Solid arrowhead in **E** indicates maternal decidual cell. The detection of cytokeratin (**F**) and vimentin (**G**) was performed in consecutive sections in order to make it easier to differentiate cell types within the canine placenta (i.e., endothelial, trophoblast, and decidual cells). Trophoblast cells stain positively for cytokeratin (open arrows [**F**]), and endothelial cells (open arrowheads [**G**]), and decidual cells (solid arrowheads [**G**]) stain positively for vimentin. There is no background staining in the isotype control (inset [**J**]).

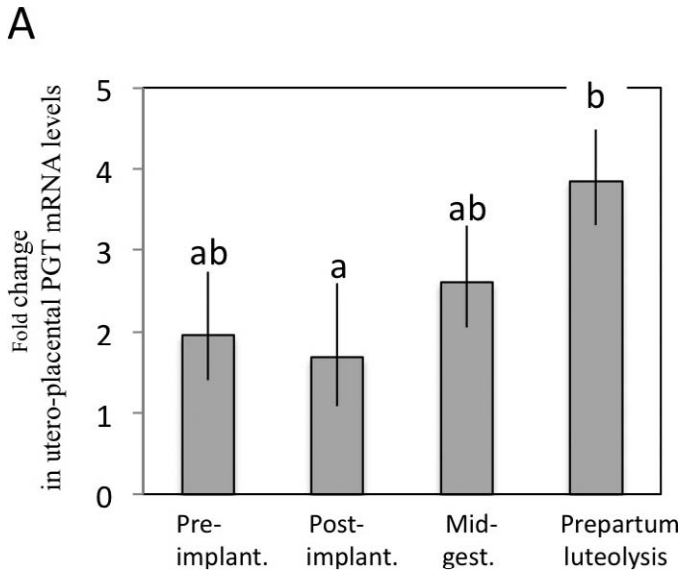

FIG. 7. Mean ± SD expression of prostaglandin transporter (*PGT*) as determined by real time (TaqMan) PCR in the canine uteroplacental units at selected time points during pregnancy. Bars with different letters differ at $P < 0.05$.

protein and 25.15 ± 2.98 ng/ μg protein, within 10 min for the uterine compartments at placentation sites and the placenta, respectively. No activity was detected in samples from which the cofactor NADPH was omitted. Further detailed investigations on enzyme kinetics were not within the scope of the present study.

Spatiotemporal, Uteroplacental Expression of PTGER2 (EP2), PTGER4 (EP4), and PGT

Both the PTGER2 (EP2) and PTGER4 (EP4) proteins were clearly detectable in the uteroplacental compartments at all time points investigated. The expression of PTGER4 was time-dependent ($P = 0.03$) and was significantly decreased ($P < 0.05$) during prepartum luteolysis (Fig. 4B). A similar expression pattern was observed for PTGER2 expression, but due to very high individual variations, the effects observed were statistically not significant ($P = 0.11$) (Fig. 4A). The specific signals of either of the proteins were significantly diminished when the antibodies were blocked with epitope-specific blocking peptides (Fig. 4, A and B).

At the cellular level, as determined by IHC, during preimplantation, PTGER2 and PTGER4 were localized to the endometrial surface epithelium, superficial and deep uterine glands, and myometrium (Figs. 5, A and B, and 6, A and B). After implantation, during mid-gestation and during prepartum luteolysis, a similar localization pattern was seen for both receptors in the uterine parts of the uteroplacental compartments (i.e., superficial uterine glands, the so-called glandular chambers) and deep uterine glands (Figs. 5, C, D, H, and I, and 6, C, D, H, and I). Furthermore, immunoreactive signals for both receptors were detected in uterine stromal cells (Figs. 5, C and D, and 6, C and D). Following placentation, anti-pan-cytokeratin and anti-vimentin staining were performed in consecutive sections in order to more easily distinguish between cell types within the canine placenta (i.e., endothelial, trophoblast and decidual cells (Figs. 5, F and G, and 6, F and G). In the placental labyrinth, stronger signals were localized in the fetal trophoblast cells, especially in the syncytiotrophoblast and invading columnar trophoblast at the base of the placental labyrinth, whereas weaker signals were observed in maternal stroma-derived decidual cells and endothelial cells (Figs. 5, E and J, and 6, E and J).

Because the anti-PGT antibody proved unsuitable for Western blot analysis, the quantitation of gene expression was performed by using semi-quantitative PCR. Consequently, *PGT* mRNA expression was detected at all selected time points during canine gestation, revealing a significant effect of time ($P < 0.02$). Its expression was more or less constant until mid-gestation, then showed significantly ($P < 0.05$) elevated levels prior to parturition, during prepartum luteolysis (Fig. 7). The protein was colocalized with PTGES, PTGER2, and PTGER4 in the endometrial superficial and deep uterine glands, vascular endothelial cells (Fig. 8, A and B), and prior to implantation, in the endometrial surface (luminal) epithelial cells; strong signals were localized in the myometrium (Fig. 8B). Following implantation and placentation endometrial signals in the uteroplacental compartment were maintained in the superficial uterine glands (the so-called glandular chambers), deep uterine glands, and vascular endothelial cells (Fig. 8, C and D). Similar endometrial localization patterns were observed during prepartum luteolysis (Fig. 8, F and G). The placental signals were predominantly localized in the fetal trophoblast cells (Fig. 8E) and weaker signals or no signals were localized in maternal decidual cells. Additionally, at the time of prepartum luteolysis, clearly visible signals were localized in maternal decidual cells (Fig. 8H). A similar signal localization pattern was observed at the mRNA level by in-situ hybridization (Fig. 9, A–E).

DISCUSSION

Although the acute luteolytic mechanism in pregnant dogs is associated with a strong increase in circulating prostaglandin F2α (PGF2α) levels in maternal peripheral blood, information is still very restricted concerning the respective biosynthetic pathways responsible for its production. Our recent investigations suggested that mechanisms not involving increased PGFS/AKR1C3 may participate in this process [7]. Coinciding with the decreased availability of PGFS/AKR1C3, increased uteroplacental expression of *PTGES* mRNA at the time of prepartum luteolysis led us to speculate on possible alternative PGF2α synthetic pathways, e.g., those utilizing PGE2 as a substrate for PGF2α synthesis.

In this study, the biochemical identity of the previously cloned PTGES was confirmed. In contrast to other species (e.g., cattle or humans [24, 25]), where at least two isoforms of this enzyme are known (i.e., the constitutively expressed cytoplasmic and inducible microsomal isoforms), this is the only canine-specific PTGES known so far. Based on its subcellular localization bound to the ER, presented herein, it appears to be a microsomal protein.

Generation and validation of a canine-specific custom-made anti-PTGES antibody allowed us to investigate the cellular distribution pattern of PTGES within the canine uteroplacental compartments. It was abundantly expressed in decidualizing uterine tissues and localized both in the glandular compartments and the uterine stroma. This is in agreement with previous observations in other species (e.g., rats [26] and pigs [27]) and with the recently reported higher expression of PTGES in early pregnant versus nonpregnant bitches [28], therefore indicating an active role for the PTGES-derived PGE2 during canine decidualization. Moreover, an essential role of PGE2-dependent mechanisms in controlling the transformation of stromal to decidual cells, and thereby regulating implantation, has been suggested for the mouse uterus [29, 30].

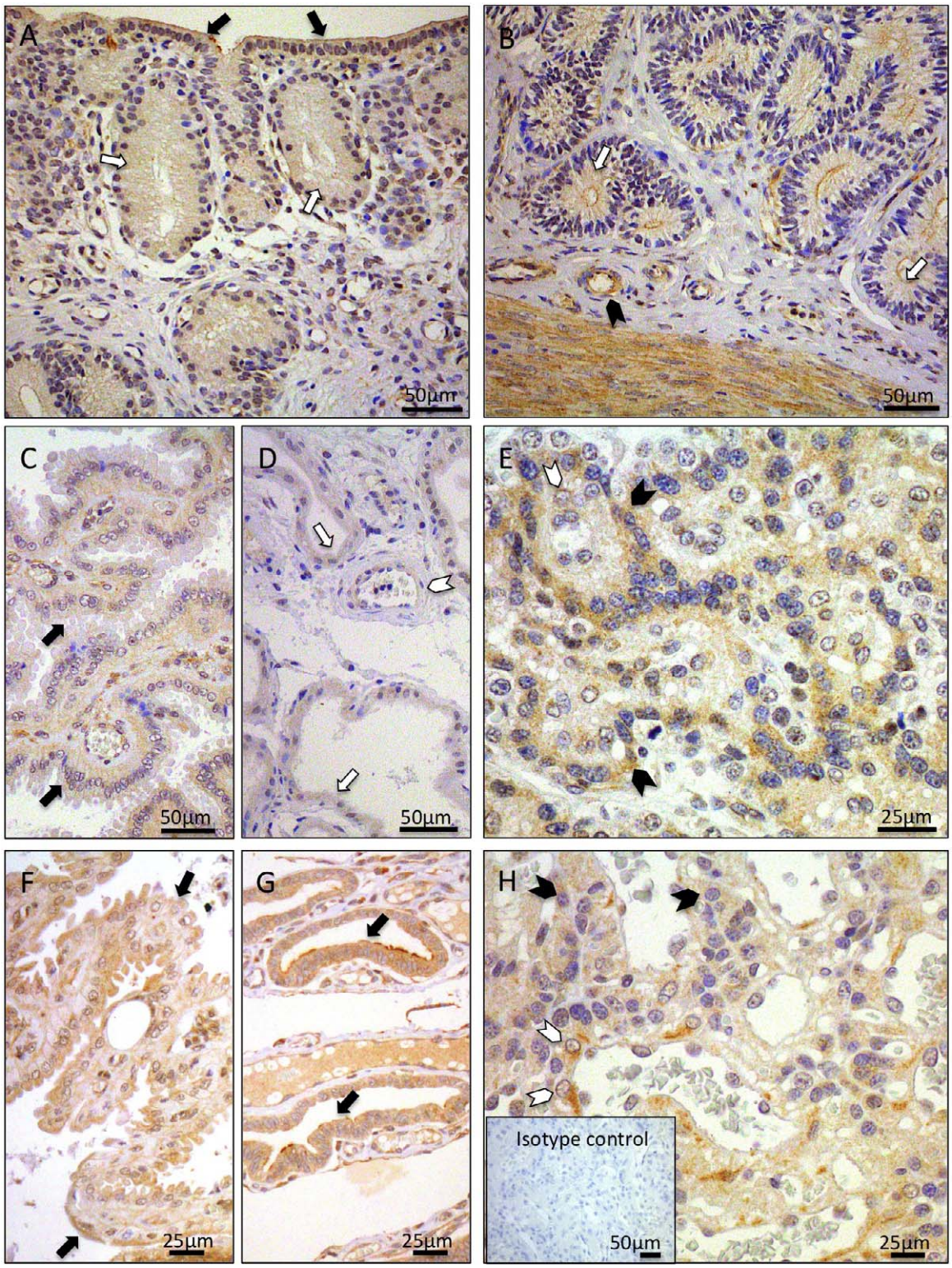

FIG. 8. Immunohistochemical localization of prostaglandin transporter (PGT) in the canine pregnant uterus at selected periods of pregnancy. Preimplantation stage (**A** and **B**), uteroplacental compartments postimplantation (**C**–**E**), and the uteroplacental compartments during prepartum luteolysis (**F**–**H**). **A**) Preimplantation endometrial PGT expression is localized to the surface (luminal) epithelial cells (weaker signals, solid arrows [**A**]), glandular epithelial cells of the superficial glands and deep uterine glands (weaker signals, open arrows [**A** and **B**]) and vascular endothelial cells (solid arrowhead [**B**]). Following implantation, within the uteroplacental compartments, endometrial signals are localized to the superficial uterine glands (the so-called glandular chambers) (solid arrows [**C**]), deep uterine glands (open arrows [**D**]), media of vessels and vascular endothelial cells (open arrowhead [**D**]). A similar endometrial localization pattern is observed during prepartum luteolysis; pointed out are superficial endometrial glands (glandular chambers) (solid arrows [**F**]) and deep uterine glands (solid arrows [**G**]). In the placental labyrinth, fetal trophoblast cells (solid arrowheads [**E** and **H**]) and maternal decidual cells (open arrowheads [**E** and **H**]) stain positively for PGT. There is no background staining in the isotype control (inset [**H**]).

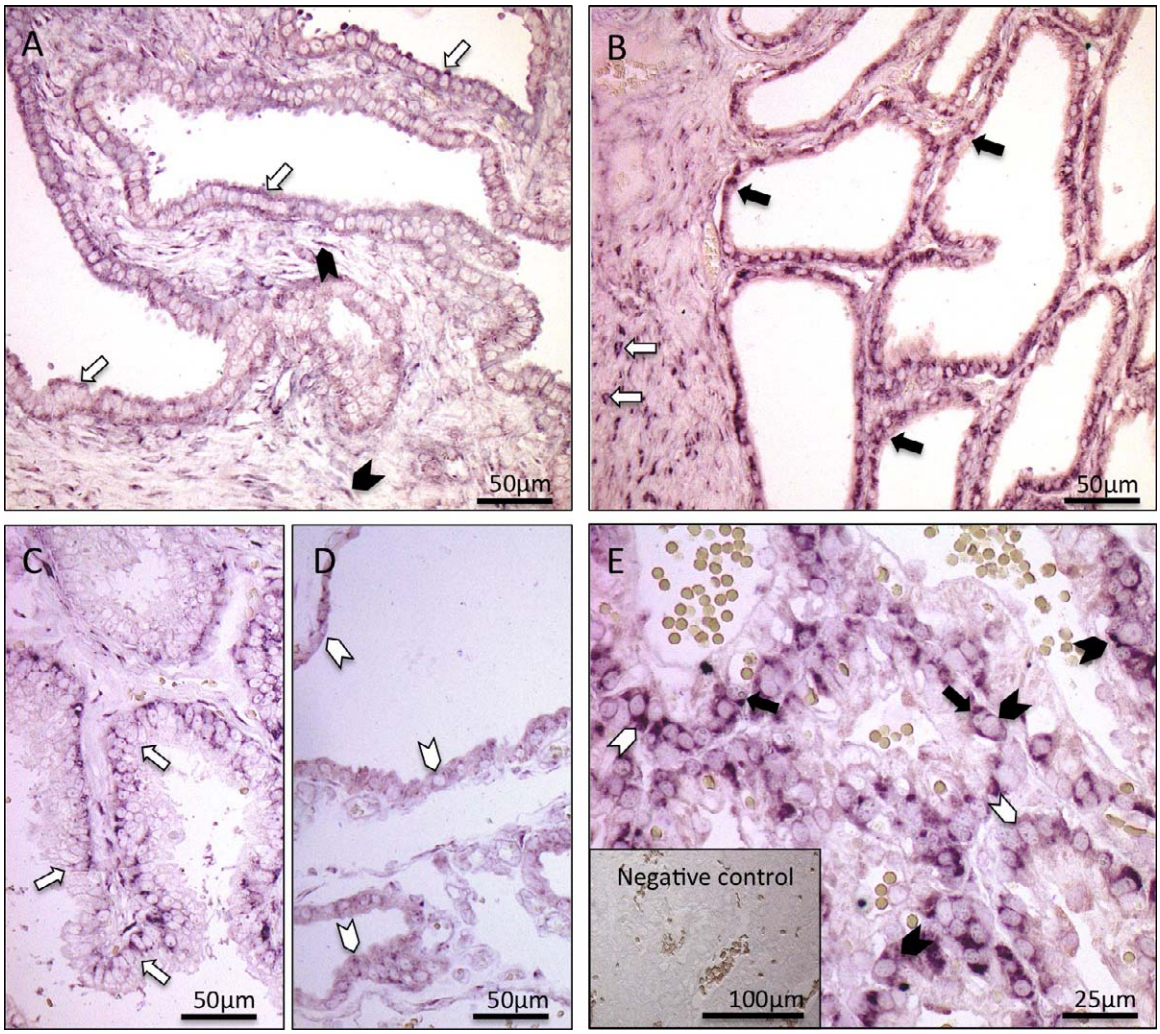

FIG. 9. Localization of prostaglandin transporter (*PGT*) mRNA as determined by in situ hybridization in the uteroplacental compartments during mid-gestation (**A** and **B**) and prepartum luteolysis (**C–E**). **A**) Signals are localized to the superficial uterine glands (open arrows) and endometrial stromal cells (solid arrowheads). **B**) Signals are localized to the deep uterine glands (solid arrows) and myocytes (open arrows). A similar endometrial localization pattern was observed during prepartum luteolysis; pointed out are superficial endometrial glands (glandular chambers; open arrows [**C**]) and deep uterine glands (open arrowheads [**D**]). **E**) The placental expression of PGT mRNA during prepartum luteolysis, localized in the fetal trophoblast cells (open arrowheads), maternal decidual cells (solid arrowheads) and capillary pericytes (solid arrows). There is no background staining in the negative control (inset to **E**).

Placental expression of PTGES mirrored its previously reported messenger localization [14] and, following implantation, was predominantly targeted to the fetal trophoblast cells, both cyto- and syncytiotrophoblasts. Colocalization of PTGES with the respective PGE2 receptors PTGER2 and PTGER4 in these cells and their upregulated protein levels in the early and mid-term placenta imply a contribution of PGE2 to the processes of placental development and/or fetal invasion. Taking into account the anticipated role of PGE2 during placental development, expression of the PTGES, PTGER2, and PTGER4 proteins in the placenta materna (i.e., in decidual and/or endothelial cells), even though weaker than in the fetal compartment, merits further investigations.

Prepartum luteolysis was associated with strongly increased uteroplacental expression of *PGT*. Its cellular colocalization with the PG system in the placenta foetalis [7, 14], as well as localization in the placenta materna, especially in decidual cells, indicate the involvement of PGT in the PG-mediated paracrine and/or endocrine signaling cascade during canine parturition. This is consistent with observations made in ruminants, where endometrial PGT expression was upregulated at the time of luteolysis [31, 32].

Concerning prepartum luteolysis, the clearly detectable expression of PTGES in fetal trophoblast resembles the situation reported for human placenta, in which strong expression of microsomal PTGES was detected in the syncytiotrophoblast at labor [25, 33]. In addition to acting on cervical softening prior to and during uterine contractile activity triggered by PGF2α [34, 35], the involvement of PGE2 in final placental maturation and release appears plausible.

Furthermore, as shown in cattle [36] and further elaborated elsewhere [15, 16], PGE2 could serve as a substrate for PGF2α synthesis due to 9-keto-PG E2 reductase (9K-PGR, CBR1) activity. The PGE2-to-PGF2α conversion pathway also appears to be important for initiation of human labor, where the enhanced conversion of PGE2-to-PGF2α due to the 9K-PGR activity seems to be one of the pathways involved in the cortisol-mediated PGF2α production in amnion fibroblast cells [37]. In this context, the most interesting discovery from our

study is the observation of the enzymatic 9K-PGR activity of microsomal fractions isolated from the prepartum dog uterus and placenta that use PGE2 for PGF2α synthesis. In the dog, the mechanisms regulating the prepartum PGF2α output are still not fully understood. The elevated cortisol levels observed in maternal peripheral blood, however, are not mandatory for normal parturition but may reflect increase in fetal cortisol at that time [2, 38]. Less is known about the local effects of cortisol at the fetoplacental and uterine levels. Nevertheless, the increased 9K-PGR activity during prepartum luteolysis could be an important regulatory mechanism facilitating PGF2α output. Further investigations are needed to identify and characterize the respective canine-specific enzyme/s responsible for this activity.

In conclusion, the changes described in the uteroplacental expression of PGT, PTGER2/EP2, and PTGER4/EP4 at selected time points of pregnancy indicate their autocrine and paracrine involvement during canine decidualization and placentation. The biochemical activity of canine PTGES toward PGE2 synthesis has been confirmed. Its subcellular colocalization with the microsomal 9K-PGR activity at the time of the COX2-dependent increase in prostanoid substrate generation during prepartum luteolysis [14] implies its possible involvement in the endocrine cascade leading to increased output of PGF2α prior to and during canine parturition.

ACKNOWLEDGMENT

The skillful technical assistance of Elisabeth Högger, Elisabeth M. Schraner, and Stefanie Ihle was greatly appreciated. The authors are grateful to Dr. Barry Bavister for careful editing of the manuscript. Part of the laboratory work was performed using the logistics at the Center for Clinical Studies, Vetsuisse Faculty, University of Zurich.

REFERENCES

1. Concannon PW, McCann JP, Temple M. Biology and endocrinology of ovulation, pregnancy and parturition in the dog. J Reprod Fertil Suppl 1989; 39:3–25.
2. Hoffmann B, Hoveler R, Nohr B, Hasan SH. Investigations on hormonal changes around parturition in the dog and the occurrence of pregnancy-specific non conjugated oestrogens. Exp Clin Endocrinol 1994; 102: 185–189.
3. Nohr B, Hoffmann B, Steinetz BE. Investigation of the endocrine control of parturition in the dog by application of an antigestagen. J Reprod Fertil Suppl 1993; 47:542–543.
4. Steinetz BG, Goldsmith LT, Harvey HJ, Lust G. Serum relaxin and progesterone concentrations in pregnant, pseudopregnant, and ovariectomized, progestin-treated pregnant bitches: detection of relaxin as a marker of pregnancy. Am J Vet Res 1989; 50:68–71.
5. Concannon PW. Biology of gonadotrophin secretion in adult and prepubertal female dogs. J Reprod Fertil Suppl 1993; 47:3–27.
6. Hoffmann B, Hoveler R, Hasan SH, Failing K. Ovarian and pituitary function in dogs after hysterectomy. J Reprod Fertil 1992; 96:837–845.
7. Gram A, Buchler U, Boos A, Hoffmann B, Kowalewski MP. Biosynthesis and degradation of canine placental prostaglandins: prepartum changes in expression and function of prostaglandin F2alpha-synthase (PGFS, AKR1C3) and 15-hydroxyprostaglandin dehydrogenase (HPGD). Biol Reprod 2013; 89:2.
8. Kowalewski MP, Fox B, Gram A, Boos A, Reichler I. Prostaglandin E2 functions as a luteotrophic factor in the dog. Reproduction 2013; 145: 213–226.
9. Kowalewski MP, Mutembei HM, Hoffmann B. Canine prostaglandin E2 synthase (PGES) and its receptors (EP2 and EP4): expression in the corpus luteum during dioestrus. Anim Reprod Sci 2008; 109:319–329.
10. Kowalewski MP, Schuler G, Taubert A, Engel E, Hoffmann B. Expression of cyclooxygenase 1 and 2 in the canine corpus luteum during diestrus. Theriogenology 2006; 66:1423–1430.
11. Hoffmann B, Buesges F, Engel E, Kowalewski MP, Papa PC. Regulation of corpus luteum-function in the bitch. Reprod Domest Anim 2004; 39: 232–240.
12. Kowalewski MP. Endocrine and molecular control of luteal and placental function in dogs: a review. Reprod Domest Anim 2012; 47(Suppl 6): 19–24.
13. Kowalewski MP. Luteal regression vs. prepartum luteolysis: regulatory mechanisms governing canine corpus luteum function. Reprod Biol 2014; 14:89–102.
14. Kowalewski MP, Beceriklisoy HB, Pfarrer C, Aslan S, Kindahl H, Kucukaslan I, Hoffmann B. Canine placenta: a source of prepartal prostaglandins during normal and antiprogestin-induced parturition. Reproduction 2010; 139:655–664.
15. Madore E, Harvey N, Parent J, Chapdelaine P, Arosh JA, Fortier MA. An aldose reductase with 20 alpha-hydroxysteroid dehydrogenase activity is most likely the enzyme responsible for the production of prostaglandin f2 alpha in the bovine endometrium. J Biol Chem 2003; 278:11205–11212.
16. Asselin E, Fortier MA. Detection and regulation of the messenger for a putative bovine endometrial 9-keto-prostaglandin E(2) reductase: effect of oxytocin and interferon-tau. Biol Reprod 2000; 62:125–131.
17. Kowalewski MP, Meyer A, Hoffmann B, Aslan S, Boos A. Expression and functional implications of peroxisome proliferator-activated receptor gamma (PPARgamma) in canine reproductive tissues during normal pregnancy and parturition and at antiprogestin induced abortion. Theriogenology 2011; 75:877–886.
18. Amoroso EC. Placentation In: Parkes AS (ed.), Marshall's Physiology of Reproduction. London: Longmans Green: 1952; 127–316.
19. Kehrer A. Zur Entwicklung und Ausbildung des Chorions der Placenta zonaria bei Katze, Hund und Fuchs. Anat Embryol (Berl) 1973; 143: 25–42.
20. Laimbacher A. Open reading frame O9 of ovine herpesvirus 2 encodes a Bcl-2 homolog which targeted the mitochondria. University of Zurich, Zurich Switzerland; 2006. Thesis.
21. Kowalewski MP, Dyson MT, Boos A, Stocco DM. Vasoactive intestinal peptide (VIP)-mediated expression and function of steroidogenic acute regulatory protein (StAR) in granulosa cells. Mol Cell Endocrinol 2010; 328:93–103.
22. Sprekeler N, Kowalewski MP, Boos A. TRPV6 and calbindin-D9k-expression and localization in the bovine uterus and placenta during pregnancy. Reprod Biol Endocrinol 2012; 10:66.
23. Kowalewski MP, Mason JI, Howie AF, Morley SD, Schuler G, Hoffmann B. Characterization of the canine 3beta-hydroxysteroid dehydrogenase and its expression in the corpus luteum during diestrus. J Steroid Biochem Mol Biol 2006; 101:254–262.
24. Parent J, Fortier MA. Expression and contribution of three different isoforms of prostaglandin E synthase in the bovine endometrium. Biol Reprod 2005; 73:36–44.
25. Meadows JW, Eis AL, Brockman DE, Myatt L. Expression and localization of prostaglandin E synthase isoforms in human fetal membranes in term and preterm labor. J Clin Endocrinol Metab 2003; 88:433–439.
26. Kennedy TG. Evidence for a role for prostaglandins in the initiation of blastocyst implantation in the rat. Biol Reprod 1977; 16:286–291.
27. Waclawik A, Rivero-Muller A, Blitek A, Kaczmarek MM, Brokken LJ, Watanabe K, Rahman NA, Ziecik AJ. Molecular cloning and spatiotemporal expression of prostaglandin F synthase and microsomal prostaglandin E synthase-1 in porcine endometrium. Endocrinology 2006; 147: 210–221.
28. Kautz E, Gram A, Aslan S, Ay SS, Selcuk M, Kanca H, Koldas E, Akal E, Karakas K, Findik M, Boos A, Kowalewski MP. Expression of genes involved in the embryo-maternal interaction in the early pregnant canine uterus. Reproduction 2014; 147:703–717.
29. Pakrasi PL, Jain AK. Cyclooxygenase-2 derived PGE2 and PGI2 play an important role via EP2 and PPARdelta receptors in early steps of oil induced decidualization in mice. Placenta 2008; 29:523–530.
30. Ni H, Sun T, Ding NZ, Ma XH, Yang ZM. Differential expression of microsomal prostaglandin E synthase at implantation sites and in decidual cells of mouse uterus. Biol Reprod 2002; 67:351–358.
31. Banu SK, Lee J, Satterfield MC, Spencer TE, Bazer FW, Arosh JA. Molecular cloning and characterization of prostaglandin (PG) transporter in ovine endometrium: role for multiple cell signaling pathways in transport of PGF2alpha. Endocrinology 2008; 149:219–231.
32. Banu SK, Arosh JA, Chapdelaine P, Fortier MA. Molecular cloning and spatiotemporal expression of the prostaglandin transporter: a basis for the action of prostaglandins in the bovine reproductive system. Proc Natl Acad Sci U S A 2003; 100:11747–11752.
33. Meadows JW, Pitzer B, Brockman DE, Myatt L. Differential localization of prostaglandin E synthase isoforms in human placental cell types. Placenta 2004; 25:259–265.

34. Fuchs AR, Goeschen K, Rasmussen AB, Rehnstrom JV. Cervical ripening and plasma prostaglandin levels. Comparison of endocervical and extra-amniotic PGE2. Prostaglandins 1984; 28:217–227.
35. Stys SJ, Dresser BL, Otte TE, Clark KE. Effect of prostaglandin E2 on cervical compliance in pregnant ewes. Am J Obstet Gynecol 1981; 140: 415–419.
36. Kankofer M. The enzymes responsible for the metabolism of prostaglandins in bovine placenta. Prostaglandins, Leukot Essent Fatty Acids 1999; 61:359–362.
37. Guo C, Wang W, Liu C, Myatt L, Sun K. Induction of PGF2alpha synthesis by cortisol through GR dependent induction of CBR1 in human amnion fibroblasts. Endocrinology 2014; 155:3017–3024.
38. Concannon PW, Butler WR, Hansel W, Knight PJ, Hamilton JM. Parturition and lactation in the bitch: serum progesterone, cortisol and prolactin. Biol Reprod 1978; 19:1113–1118.